

Electro-Explosive Mechanism of Carbon Cathode Destruction in Negative Corona Discharge in Trichel Pulse Regime

Alexey A. PETROV, Ravil H. AMIROV, Erik I. ASINOVSKII and Igor S. SAMOYLOV

Joint Institute for High Temperatures of Russian Academy of Sciences

(Received: 2 September 2008 / Accepted: 25 November 2008)

Erosion of the graphite cathode has been investigated in point-to-plane negative corona discharge in ambient air. Oscillography of discharge current and observation of cathode spot dynamics as well as electron micrography of the cathode surface has been performed. An attempt was made to explain cathode erosion in terms of local electro-explosions caused by pulsed discharge current. Difference of erosion pattern of the graphite cathode in Trichel pulse corona and pulseless glow corona was found.

Keywords: cathode erosion, Trichel pulses, glow corona, electro-explosion.

1. Introduction

Cathode erosion in negative corona discharge was first observed in 1940 by Bennet [1] on W cathodes. Weissler [2] investigated erosion on W, Pt, Cu, Al and Pb point cathodes and came to the conclusion that erosion was due to bombardment of the surface by positive ions. However the energy of positive ions in negative corona was estimated as 1 eV and insufficient for cathode sputtering [2,3]. So in works [3-5] cathode erosion was attributed to the chemical action of discharge. In work [6] cathode erosion was explained in terms of dielectric layers disruption because of skin charging by positive ions and due to photoeffect. In [7] erosion of the cathode in negative corona is associated with ecton processes. So the conclusion is that there is not any conventional model of cathode erosion in negative corona discharge.

Erosion of the cathode in Trichel pulse negative corona should be associated with phases of discharge behavior – that is with Trichel pulses. First extensive study of these pulses with typical amplitude 1 mA, period 1 μ s and FWHM 10 ns was performed by Trichel.

In different numerical models of Trichel pulses [8-15] surface processes of secondary electron emission, photoemission and field emission are generally involved. In the gap the main considered process was the propagation of cathode-directed ionization wave [16]. According to simulation results performed in [9] movement of this wave corresponds to the leading edge of the Trichel pulse and the electric field magnitude on the cathode surface may reach 10^6 V/cm. However in spite of very different cathode processes included in the simulation models a good correspondence between the calculated and measured waveforms of Trichel pulses was demonstrated. So actually there is not any certain decision about the most probable cathode processes in negative corona.

e-mail: lioha84@mail.ru

The aim of this work is investigation of the cathode erosion mechanism. An attempt was made to explain cathode erosion in terms of local electro-explosions caused by pulsed discharge current. Character of the graphite cathode erosion in glow corona and Trichel pulse corona is compared.

2. Experimental setup and procedure

Negative corona discharge has been investigated in point-to-plane electrode configuration in atmospheric pressure air both in Trichel pulse and pulseless mode. As a cathode pointed graphite pins with diameter 50-300 μ m were taken. Spectral graphite S-3 was used. Pins were mechanically made and shaped by use of diamond abrasive. No performance was made to shape the pins tip before discharge because it was shaped and conditioned in few seconds due to erosion processes after the discharge was switched on.

Cathode axis was perpendicular to the anode plane and discharge gap was adjusted from 10 to 30 mm. Positive voltage in the range 8-15 kV was supplied to the plane anode which was a 10 cm diameter silicon disc. Trichel pulses were registered by S1-75 dial oscilloscope with 300 MHz bandwidth which was connected across a 50 Ohm resistor between the cathode and the ground. Average discharge current was registered by use of dial ammeter between the anode and power supply. Cathode surface was observed by means of telemicroscope with spatial resolution 5 μ m.

Topography of cathode surface after treatment in the discharge was analyzed with spatial resolution 40 nm by use of FEI Quanta 200 scanning electron microscope.

3. Results and discussion

It was found that Trichel pulse train with constant amplitude and pulse time separation was implemented when discharge did not change its position on the cathode surface for a certain time. When discharge changes its position on the cathode surface amplitude and pulse time separation of Trichel pulses may change, increase of amplitude results in increase of the pulse time separation and conversely. The average discharge current does not change upon the wandering of the discharge spot position on the cathode surface. Fig.1 shows the typical oscillogram of the Trichel pulses.

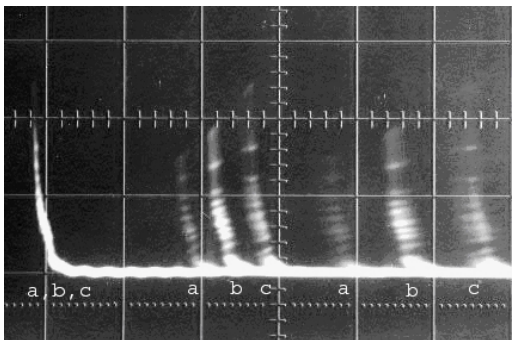


Fig.1 Typical oscillogram of discharge current. Three pulse trains (a, b, c) may be distinguished. Frame exposition 40 ms. Each train is characterized by its own nearly stable amplitude and period.

This photograph includes about 10^4 oscilloscope sweeps following each other during 40 ms. The beginning of each oscilloscope sweep coincides with the beginning of one of the Trichel pulses. Voltage, average discharge current and discharge gap are fixed. Three trains of current pulses denoted a, b, and c can be separated on the photograph so that each train is characterized by individual nearly stable amplitude and pulse time separation. Side observation of the cathode surface revealed at least three stable fixations of cathode spot on the cathode surface at this moment. Using such oscillograms we can draw amplitude-pulse time separation diagrams of Trichel pulses. An example of such diagram for 50 μm and 300 μm -diameter cathodes is represented on the Fig.2. Experimental points which are connected by a line correspond to various cathode spot positions at fixed discharge current, gap, voltage and cathode diameter. Shift of a line is caused by change of cathode diameter or gap properties. So this diagram let separate influence of surface conditions from influence of gap properties on the Trichel pulse parameters. Also it demonstrates that amplitude of Trichel pulses increases from 1 mA to 30 mA as a result of cathode diameter rise from 50 μm to 300 μm .

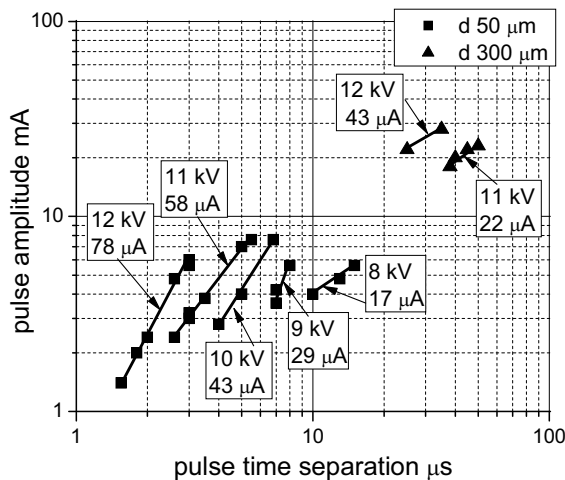


Fig.2 Amplitude-pulse time separation diagrams for 50 μm diameter and 300 μm diameter graphite cathodes. Discharge gap 10 mm.

Erosion rate of graphite cathodes in different experiments was varied in the range $10^{-5} - 2 \cdot 10^{-4}$ g/coul. This is approximately 2 orders of magnitude more than for metal cathodes. No simple dependence between cathode diameter, discharge current and erosion rate was found.

Graphite surface before treatment in discharge is demonstrated on the Fig.3 – this surface is a break of the cathode and was not subjected to any other mechanical treatment. This is polycrystalline graphite with typical grain size 1 μm .

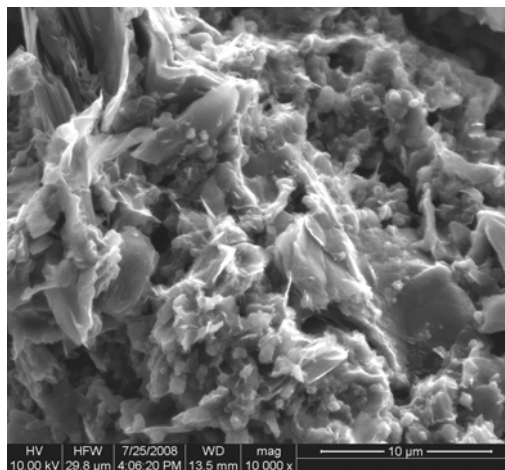


Fig.3 Graphite before treatment in negative corona.

Tip of 50 μm diameter graphite pin is demonstrated on the Fig.4. This erosion pattern is typical for graphite cathodes of all diameters after treatment in Trichel pulse corona. Surface of such cathode is covered by numerous erosion pores.

Tip of 70 μm diameter graphite cathode after

treatment in pulseless corona is demonstrated on the Fig.5. Its surface is mostly striated by numerous fissures 1 μm thickness and 20 μm longwise. Also on the surface three 50 μm size cavities are observed. On the 150 μm diameter graphite cathode which is demonstrated on the Fig.6 four such cavities were found after treatment at the same average current 100 μA in pulseless glow corona.

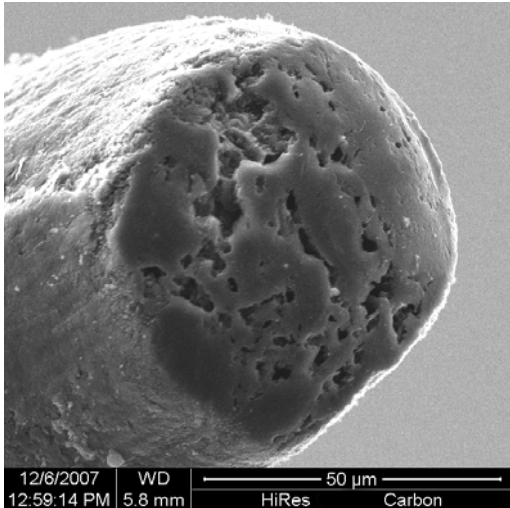


Fig.4 Graphite pin after treatment in Trichel pulse corona. Discharge current 50 μA

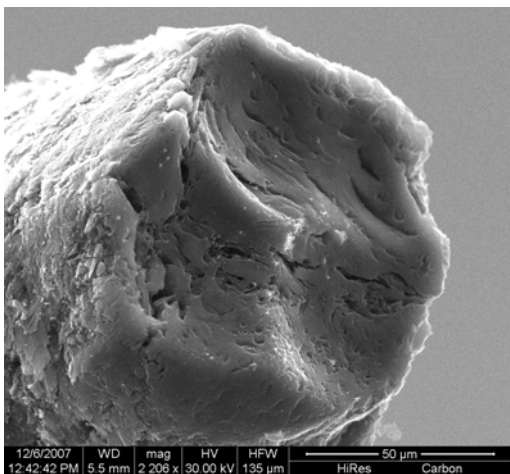


Fig.5 Graphite pin after treatment in pulseless negative corona. Discharge current 100 μA .

In Trichel pulse negative corona concentrated energy release on the cathode surface which causes erosion is associated with interaction between the charged head of cathode-directed streamer and the cathode surface. This streamer is registered as a leading edge of Trichel pulse. Calculation of the electric field strength induced by streamers near cathode surface was made in [9] – pulsed field on the microareas may reach 10^6 V/cm. Microasperities present on the surface may further increase it in 10-1000 times. Thus, the self-oscillatory regime of cathode-directed streamers creates microareas

of high local pulsed electric field which sequentially arise on the pointed cathode surface for a time of the order 10^{-9} s. Eventually this result in field emission culminating in microexplosions on the cathode surface.

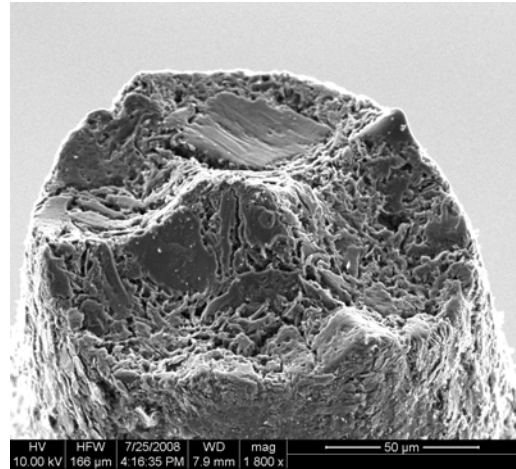


Fig.6 Graphite pin after treatment in pulseless corona. Discharge current 100 μA .

Let us estimate the value of integral of specific current action [7] of Trichel pulse which characterizes nanosecond Joule energy delivery in the cathode microerosion center and may serve as a criterion of microexplosive processes. We assume that Trichel pulse causes ejection of a single spherical erosion fragment of the cathode surface and current on the cathode surface closes through the cross-section of this erosion fragment. To estimate current density j we define the size of an erosion fragment as the ratio of the cathode total erosion to the number of Trichel pulses. The amount of erosion was determined by comparison of the cathode micrographs taken before and after discharge by use of scanning microscope.

For 300 μm diameter graphite cathode an elementary erosion fragment was measured as 10^6 nm^3 and accordingly the cross-section of elementary erosion fragment and elementary microcrater was $2 \cdot 10^{-10}$ cm^2 . At Trichel pulse current amplitude of 25 mA the maximal current density is no less than 10^8 A/cm^2 . Setting the FWHM of a Trichel pulse equal to $t=10$ ns we can calculate integral of its specific current action:

$$h = \int_0^t j^2 dt \approx 10^8 \text{ A}^2 \text{ s} / \text{cm}^4 \quad (1)$$

This value indicates that erosion in Trichel pulse negative corona can be associated with microexplosive processes [7]. However on 50 μm diameter pin amplitude of Trichel pulses is about 1 μA and the value of integral of specific current action of Trichel pulse is approximately 10^6 $\text{A}^2 \text{ cm}^{-4} \text{ s}$. Hence the conclusion is that

some additional mechanisms of cathode erosion are possible.

There is a number of arguments in favor of electro-explosion mechanism of cathode erosion in Trichel pulse corona:

a) No gas or cathode material was ever found in which erosion had not occurred. This reason does not contradict to microexplosive erosion mechanism however excludes chemical action as the main cause of erosion.

b) Energy of positive ions in negative corona was estimated as 0.01-1 eV [2,3,17] and insufficient for sputtering. However in [18] this energy was estimated as 10 eV; so there is not any certain decision about its value.

c) Action of discharge on cathode surface in Trichel pulse regime is confined in time and space because 100 nm size craters on the cathode surface are observed (Fig.4) and discharge current is represented as succession of 10 ns pulses. So we can say about high energy density processes on the cathode surface. This argues in favor of microexplosions.

4. Conclusions

Results of oscillography of Trichel pulses which are presented in form of amplitude-pulse time separation diagrams let separate influence of cathode spot wandering from influence of gap properties on Trichel pulses. Difference of erosion pattern of the graphite cathode in Trichel pulse corona and pulseless glow corona was found. Value of integral of specific current action of Trichel pulse argues in favor of electro-explosions on the cathode surface as the cause of erosion.

5. Acknowledgements

The authors would like to thank the employee of the Research Educational Center "Nanotechnology" at Moscow Institute of Physics and Technology for affording the opportunity of working on scanning electron microscope FEI Quanta 200 as well as on probe microscopes.

- [1] W.H. Bennet, Phys. Rev. **58**, 992 (1940).
- [2] G.L. Weissler, Phys. Rev. **63**, 96 (1943).
- [3] J. M. Meek and J.D. Craggs, Electrical Breakdown of Gases, Clarendon Press, Oxford, UK, (1953).
- [4] A. Greenwood, Phys. Rev. **88**, 91 (1952).
- [5] A. Goldman et al., Proceedings of the 8th International Conference on Gas Discharges and Their Applications, Oxford 469 (1985).
- [6] H. Korge et al., J. Phys. D: Appl. Phys. **26**, 231 (1993).
- [7] G.A. Mesyats, Phys. Usp. **38**, 567 (1995).
- [8] R. Morrow, Phys. Rev. A. **32**, 3821 (1985).

- [9] A.P. Napartovich et al., J. Phys. D: Appl. Phys. **30**, 2726 (1997).
- [10] T. Rees and J. Paillol, J. Phys. D: Appl. Phys. **30**, 3115 (1997).
- [11] D.K. Gupta, S. Mahajan and P.I. John, J. Phys. D: Appl. Phys. **33**, 681 (2000).
- [12] J. Liu and G.R. Raju, IEEE Transactions on Dielectrics and Electrical Insulations, **1**, 520 (1994).
- [13] C. Soria-Hoyo, F. Pontiga and A. Castellanos, J. Phys. D: Appl. Phys. **40**, 4552 (2007).
- [14] L. Salaso et al., J. Appl. Phys. **58**, 2949 (1985).
- [15] J.M.K. Mac Alpine and W.C. Yim, Conf. on electrostatical insulations and dielectric phenomena, 118 (1995).
- [16] M. Cernak, T. Hosokawa and I.J. Odobina, Phys. D: Appl. Phys. **26**, 607 (1993).
- [17] J. Chen and H. Jane Davidson, Plasma Chemistry and Plasma Processing, **23**, 83 (2003).
- [18] W.H. Weissler, J. Appl. Phys. **23**, 844 (1952).